The Journal of Immunology

RESEARCH ARTICLE | AUGUST 01 2003

Functional Analysis of the TCR Binding Domain of Toxic Shock Syndrome Toxin-1 Predicts Further Diversity in MHC Class II/Superantigen/TCR Ternary Complexes [1]

John K. McCormick; ... et. al

J Immunol (2003) 171 (3): 1385–1392.
https://doi.org/10.4049/jimmunol.171.3.1385

Functional Analysis of the TCR Binding Domain of Toxic Shock Syndrome Toxin-1 Predicts Further Diversity in MHC Class II/Superantigen/TCR Ternary Complexes[1]

John K. McCormick,[2]* Timothy J. Tripp,* Andrea S. Llera,[3]† Eric J. Sundberg,† Martin M. Dinges,[4]* Roy A. Mariuzza,† and Patrick M. Schlievert[5]*

Superantigens (SAGs) aberrantly alter immune system function through simultaneous interaction with lateral surfaces of MHC class II molecules on APCs and with particular variable regions of the TCR β-chain (Vβ). To further define the interface between the bacterial SAG toxic shock syndrome toxin-1 (TSST-1) and the TCR, we performed alanine scanning mutagenesis within the putative TCR binding region of TSST-1 along the central α helix adjacent to the N-terminal α helix and the β7-β9 loop as well as with two universally conserved SAG residues (Leu[137] and Tyr[144] in TSST-1). Mutants were analyzed for multiple functional activities, and various residues appeared to play minor or insignificant roles in the TCR interaction. The locations of six residues (Gly[16], Trp[116], Glu[132], His[135], Gln[136], and Gln[139]), each individually critical for functional activity as well as direct interaction with the human TCR Vβ2.1-chain, indicate that the interface occurs in a novel region of the SAG molecule. Based on these data, a model of the MHC/TSST-1/TCR ternary complex predicts similarities seen with other characterized SAGs, although the CDR3 loop of Vβ2.1 is probably involved in direct SAG-TCR molecular interactions, possibly contributing to the TCR Vβ specificity of TSST-1. ***The Journal of Immunology,*** **2003, 171: 1385–1392.**

Superantigens (SAGs)[6] (1) are a class of bacterial or viral proteins that aberrantly alter immune system function through simultaneous interaction with lateral surfaces of MHC class II molecules on APCs, and with particular variable regions of the α/β TCR (Vβ) (reviewed in Refs. 2 and 3). Although SAGs bind the TCR with affinities similar to those of typical TCR/peptide/MHC interactions (4–8), SAGs bind primarily based on specific TCR Vβ-chains without the requirement for Ag processing and can thus stimulate large fractions of both $CD4^+$ and $CD8^+$ T lymphocytes. This activity, defined as superantigenicity (1), results in the extensive activation and proliferation of T cells with the corresponding massive release of cytokines, including TNF-β, IL-2, and IFN-γ from T cells and TNF-α and IL-1 from APCs. It is the subsequent actions of these and other cytokines that are believed to mediate the pathological consequences leading to capillary leakage and the toxic shock syndrome (TSS). Ultimately, following the initial expansion, SAG-specific T lymphocytes may be rendered anergic (9).

TSS toxin-1 (TSST-1) is a bacterial SAG secreted by strains of *Staphylococcus aureus* that belongs to the pyrogenic toxin class of SAGs (3). TSST-1 has been associated with TSS since 1981 (10, 11), and it has been estimated that this exotoxin is responsible for ~50% of nonmenstrual-associated TSS cases due to *S. aureus* and essentially all cases of menstrual-associated TSS (12). This latter association is probably due to the apparently unique ability of TSST-1 among the pyrogenic toxin SAGs to cross mucosal surfaces (13). The crystal structure of this SAG (14, 15) as well as those of many others have been determined (reviewed in Ref. 2), and each shows a similar architecture, divided into two domains. The small domain (residues 18–89 in TSST-1) is composed of a five-strand mixed β-barrel, and the large domain (residues 1–17 and 90–194 in TSST-1) is built around a long central α helix (residues 125–140 in TSST-1) lying against a five-strand β-sheet. The crystal structures of MHC class II complexed with TSST-1 (16) and staphylococcal enterotoxin B (SEB) (17) have been determined, indicating that the interface occurs through the small domain within the O/B fold motif. These studies also revealed that although the binding regions of SEB and TSST-1 on MHC class II overlap, the interaction of TSST-1 is partially peptide dependent (18), while SEB binds more to the edge of the peptide binding groove of MHC class II. The crystal structure of MHC class II complexed with the high affinity, zinc-dependent binding site within the β grasp region on the large domain of streptococcal pyrogenic exotoxin C (SPE C) has also been determined, revealing extensive contacts with the class II bound peptide and indicating that the interaction of SAG with MHC class II can occur through diverse surfaces (19). Furthermore, the structure of SEH bound to HLA-DR1 revealed an interaction similar to that of SPE C although with unrelated peptides, indicating the possibility that the

*Department of Microbiology, University of Minnesota Medical School, Minneapolis, MN 55455; and †Center for Advanced Research in Biotechnology, University of Maryland Biotechnology Institute, Rockville, MD 20850

Received for publication February 20, 2003. Accepted for publication May 28, 2003.

The costs of publication of this article were defrayed in part by the payment of page charges. This article must therefore be hereby marked *advertisement* in accordance with 18 U.S.C. Section 1734 solely to indicate this fact.

[1] This work was supported by National Institutes of Health Grant AI22159 (to P.M.S.) and National Institutes of Health Grants AI36900 and AI42937 (to R.A.M.).

[2] Current address: Lawson Health Research Institute and Department of Microbiology and Immunology, University of Western Ontario, Grosvenor Campus, 268 Grosvenor Street, London, Ontario, Canada N6A 4V2.

[3] Current address: Gene Therapy Laboratory, Fundación Instituto Leloir, Buenos Aires, Argentina, 1405.

[4] Current address: Department of Medicine, University of Colorado Health Sciences Center, Denver, CO 80262.

[5] Address correspondence and reprint requests to Dr. Patrick M. Schlievert, Department of Microbiology, University of Minnesota Medical School, MMC 196, 420 Delaware Street SE, Minneapolis, MN 55455. E-mail address: pats@lenti.med.umn.edu

[6] Abbreviations used in this paper: RU, resonance units; SAG, superantigen; SEA, staphylococcal enterotoxin A; SEB, staphylococcal enterotoxin B; SEC, staphylococcal enterotoxin C; SPE A, streptococcal pyrogenic exotoxin A; SPE C, streptococcal pyrogenic exotoxin C; TSS, toxic shock syndrome; TSST-1, toxic shock syndrome toxin-1; Vβ, variable region of the TCR β-chain.

0022-1767/03/$02.00

peptide interaction is not specific, yet different peptides may modulate the affinity of this interaction (20).

The interactions between the relevant TCR β-chain with the SAGs staphylococcal enterotoxin C (SEC) (21) and SEB (22) as well as streptococcal pyrogenic exotoxin A (SPE A) and SPE C (23) have been structurally characterized. These studies have revealed that the orientations of SEB, SEC, and SPE A, when bound to their respective TCR β-chains, are highly similar (23); however, the SPE C-TCR β-chain complex had an entirely different binding mode for SAG-TCR interaction, with a more extensively buried interface and numerous specific interactions. Significantly, the SPE C/TCR complex modeled with the SPE C/MHC complex indicated a complete dissociation between the TCR and MHC molecules (23). In other work, staphylococcal enterotoxin A (SEA) has been shown to stimulate γδ T cells expressing Vγ2, similar to SAG activation of αβ T cells, and mutagenesis and domain swapping suggested that the SEA recognition site for γδ TCR was similar to the SEC recognition site for Vβ8.2 (24). Finally, TCR interaction with the SAG from *Mycoplasma arthritidis* is stabilized by the β-chain CDR3 region (25), a region not involved in other characterized SAG/TCR interactions, providing further evidence for the diversity of SAG interaction with the TCR.

The cocrystal structure of TSST-1 complexed with the human Vβ2.1 TCR (hVβ2.1) has yet to be determined, and although various residues have been implicated as important for this interaction (26–32), the structure of the TSST-1/hVβ2.1 interface remains to be characterized. In sum, these mutagenesis studies indicate that the TCR binding domain of TSST-1 resides in the cleft located along the central α helix between the N-terminal α helix and the β7-β9 loop (32) in contrast to SEB, SEC, SPE A, and SPE C, where this binding domain is located in a cleft on the other side of the molecule between the large and small domains (21–23). A key issue regarding previous TSST-1 mutagenesis studies is that each of these mutations is hypothesized to reside in the TSST-1/TCR interface because they are located outside the MHC binding domain, although direct interaction with the TCR has not been demonstrated. Our current study was designed to further define residues important for the functional interaction of TSST-1 with the TCR by alanine scanning mutagenesis. Our data suggest that residues Tyr^{13}, Ser^{15}, Leu^{137}, His^{141}, and Tyr^{144} are irrelevant for TCR recognition or play a minor stabilizing role in the interaction. Our data also indicate that residues Gly^{16}, Trp^{116}, Glu^{132}, His^{135}, Gln^{136}, and Gln^{139} are individually crucial for direct binding to hVβ2.1. Due to the location of these residues, we propose a model in which the MHC/TSST-1/TCR ternary complex is similar to the ternary complex of SEB, SEC, and SPE A, yet the TSST-1 complex may allow for direct interactions between the CDR3 loop of the TCR β-chain and TSST-1. Based on this model and in agreement with the variability of Vβ-specificity seen with different SAGs, it is likely that β-chain ligation by TSST-1 represents a distinct mode of SAG/TCR engagement.

Materials and Methods

Reagents

All chemicals were of analytical grade. Oligonucleotides were obtained from Integrated DNA Technologies (Coralville, IA). *Pfu* DNA polymerase and dNTPs were purchased from Stratagene (La Jolla, CA). Water and materials were maintained pyrogen free for all in vivo and biological activity experiments.

TSST-1 mutants

The wild-type TSST-1 gene (*tstH*; where H stands for *h*uman isolate) (33) was obtained from a chromosomal DNA preparation of *S. aureus* MN8 digested with *Hin*dIII and *Sal*I. The fragment containing *tst*H was cloned into pCE104 (a shuttle vector containing pE194 and pUC18), also digested with *Hin*dIII and *Sal*I to create pCE107. This plasmid was used to express wild-type TSST-1 from *S. aureus* RN4220 and was also used as the template for mutagenesis. Mutations were generated by the inverse PCR QuikChange mutagenesis procedure (Stratagene), and mutagenic primers are listed in Table I. The double-mutant Y115A/W116G was created because primers were based on the original published sequence that contained a mutation indicating Gly at position 116 (33) when in reality there is a Trp at this position. Mutated plasmids were transformed into *Escherichia coli* DH5α, and the *tstH* gene was sequenced to confirm that each mutation was incorporated and no second site mutations were generated. Correct plasmids were transformed into *S. aureus* RN4220 by protoplast transformation (34).

Protein purification

Mutant toxins were produced and purified from *S. aureus* RN4220 harboring recombinant plasmids as previously described (11). Briefly, strains were grown to stationary phase in pyrogen-free beef heart medium containing 5 μg/ml of erythromycin for plasmid maintenance, and culture supernatants were concentrated by precipitation with a final concentration of 80% ethanol. Precipitates were resolubilized in pyrogen-free water, and purification was achieved by preparative flatbed isoelectric focusing. The purity of the toxin preparations was assessed by SDS-PAGE.

The cDNA for RSD3 TCR was a gift from U. Utz and R.-P. Sekaly (University of Montreal, Montreal, Canada). This human TCR is specific for HTLV-I TAX_{11-19} peptide in the context of HLA-A2.1. The expression and purification of recombinant human TCR Vβ2.1Jβ2.3Dβ2.1Cβ2 (herein referred to as hVβ2.1) were accomplished as previously described (23).

T cell proliferation assays

Gradient purified human PBMCs or unfractionated rabbit spleen cells were stimulated in vitro in 96-well (2×10^5 cells/well) microtiter plates with serial 1/10 dilutions (in quadruplicate) of purified wild-type or mutant TSST-1 molecules. RPMI medium (BioWhittaker, Walkersville, MD) supplemented with 10% FCS (Sigma-Aldrich, St. Louis, MO), 100 μg/ml

Table I. *Altered amino acid residues of TSST-1 and primers used for construction of various mutants by site-directed mutagenesis*

Targeted Amino Acid	Mutant	Corresponding Primers[a]
Tyr^{13}	Y13A	5′-TTGCTAGACTGGGCCAGTAGTGGGTCT-3′
Ser^{15}	S15A	5′-GACTGGTATAGTGCCGGGTCTGACACT-3′
Tyr^{115}	Y115A	5′-AGCCCCTTAAAGGCCTGGCCAAAGTTC-3′
Try^{116}	W116A	5′-CCCTTAAAGTATGCGCCAAAGTTCGAT-3′
Tyr^{115}/Trp^{116}	Y115A/W116G	5′-AGCCCCTTAAAGGCCGGGCCAAAGTTC-3′
Leu^{137}	L137A	5′-ATTCGTCATCAGGCCACTCAAATACAT-3′
Gln^{139}	Q139A	5′-CATCAGCTAACTGCCATACATGGATTA-3′
His^{141}	H141A	5′-CTAACTCAAATAGCCGGATTATATCGT-3′
Tyr^{144}	Y144A	5′-ATACATGGATTAGCCCGTTCAAGCGAT-3′
Gly^{32}/Ser^{32}	G31S/S32P	5′-TTAGATAATTCCTTAAGTCCTATGCGTATAAAAAAC-3′

[a] Underlined bases are areas in the primer that have been mutated to elicit the corresponding amino acid mutation. A complementary primer for each primer listed here was also made to perform the mutagenesis method outlined in *Materials and Methods.*

streptomycin (Sigma-Aldrich), 100 U/ml penicillin (Sigma-Aldrich), 2 μg/ml polymyxin B (Sigma-Aldrich), and 1% L-glutamine (Sigma-Aldrich) was used as the culture medium, and cells were incubated in 7% CO_2 at 37°C. Cells were pulsed with 1 μCi/well of [^{3}H]thymidine (NEN, Boston, MA) after 72 h, and after another 18 h cells were harvested on fiberglass filters, and [^{3}H]thymidine incorporation was assessed in a scintillation counter. Background was considered counts from cells not treated with toxin.

Evaluation of binding of hVβ2.1 to TSST-1 and its mutants by surface plasmon resonance

The binding of hVβ2.1 to immobilized TSST-1 and its mutants was monitored with a BIAcore 1000 instrument (Pharmacia Biosensor, Uppsala, Sweden) (4). SAGs were coupled via amine groups to a dextran matrix on CM5 sensor chips at a total mass corresponding to ~1000 resonance units (RU). SEA or SEB in an equivalent surface density was used as the control surface, as no specific binding of hVβ2.1 chain to these SAGs was detected. The β-chain was dialyzed against 10 mM sodium-HEPES (pH 7.5), 150 mM NaCl, 3.4 mM EDTA, and 0.005% P20 surfactant (HBS-P20) and was characterized immediately before use by gel filtration and ultracentrifugation analysis to ensure that no aggregation was evident. Measurements were conducted at 25°C by injecting increasing concentrations of hVβ2.1 up to a maximum of 100 μM at a flow rate of 10 μl/min. Due to the low affinities, total dissociation was obtained with HBS-P20 washing, without the need of HCl regeneration of the binding surface. Data were analyzed using BIAevaluation software. K_d values were determined by Scatchard analysis of equilibrium binding measurements.

Animal models of TSS

Two models were used to assess the ability of the mutated toxins to induce fever and lethal shock in American Dutch belted rabbits (Birchwood Farms, WI). In the first model, miniosmotic pumps (Alza Pharmaceuticals, Palo Alto, CA) were preloaded with 200 μg of wild-type or mutated TSST-1 proteins in PBS (pH 7.2) (35). These devices are designed to release toxin at a constant rate over a period of 7 days to mimic toxin exposure during infection. Miniosmotic pumps were s.c. implanted in American Dutch belted rabbits, and three (or more) rabbits were used for each toxin preparation. Temperatures were recorded on days 0 and 2 to determine the pyrogenic activity of the mutants. Animals were monitored for symptoms of TSS, and mortality was recorded over a 10-day period. In the enhancement of endotoxin shock model (36), American Dutch belted rabbits were pretreated with low doses of wild-type or mutated TSST-1 proteins (5 μg/kg of body weight) administered i.v. by the marginal ear vein. After 4 h animals were challenged with a sublethal dose (10 μg/kg) of endotoxin from *Salmonella typhimurium*. Animals were monitored for symptoms of TSS, and mortality was recorded over 48 h. In both models, animals displaying clear signs of lethal shock were prematurely euthanized in accordance with our animal experimentation protocols. All animal experiments performed in this study have received prior approval by from University of Minnesota institutional review board.

Results

TSST-1 mutants

To further define residues important for the functional interaction of TSST-1 with the TCR, we performed alanine scanning mutagenesis of various residues located near the putative TCR binding region located along the central α helix adjacent to the N-terminal α helix and the β7-β9 loop (32). Alanine substitution was chosen because this technique removes the targeted amino acid side chain while minimizing steric or electrostatic constrains on the tertiary structure of the protein (37). Mutations encompassed residues Tyr^{13} and Ser^{15} located in the N-terminal α helix region, residues Tyr^{115} and Trp^{116} located between strands β8 and β9, and residues Leu^{137}, Gln^{139}, His^{141}, and Tyr^{144} located near the distal end of the central helix that joins the large and small domains. In this work we also included the previously constructed mutants G16V (30), which is located on the N-terminal α helix, as well as E132K and Q136A, located along the central helix (31). A control MHC class II binding mutant was also created (G31S/S32P) that lacks significant proliferative activity (30), and these residues are known to be located at the interface with the MHC class II molecule HLA-DR1 (16). The Ser^{32} mutation is believed to account for most of the impaired interaction with MHC class II (30), although other data suggest that Gly^{31} is also critical for MHC class II binding (38). All the mutant genes (Table I) were constructed using plasmid pCE107 as a template, and mutated proteins were expressed and purified from *S. aureus* RN4220. Each protein was purified to apparent homogeneity as determined by SDS-PAGE, with a typical yield of ~5 mg/liter.

Mitogenic capacity of various TSST-1 mutants

Initial experiments determined the effect of each individual mutation on superantigenic activity by measuring the ability of each protein to induce the proliferation of unfractionated rabbit splenocytes or gradient purified human PBMCs (Table II). Mitogenic

Table II. *Mitogenic capacity and dissociation constants for binding of wild-type TSST-1 and mutated proteins to the human Vβ2.1 TCR.*

TSST-1 Mutant	Mitogenic Capacity (pg/ml)[a]		Affinity Measurements[b]		
	Human	Rabbit	K_d BIAcore ($\times 10^{-6}$ M)	ΔG (kCal/mol)	ΔΔG (kCal/mol)
Wild type	50	50	2.3	−7.7	
Y13A	50	5–50	2.1	−7.7	0
S15A	50	50	1.0	−8.2	−0.5
G16V	>5,000,000	>5,000,000	NB[c]	>−5.5	>2.2
Y115A	500	50–500	13.1	−6.7	1.0
W116A	50,000	50–500	NB	>−5.5	>2.2
Y115A/W116G	>5,000,000	>5,000,000	NB	>−5.5	>2.2
E132K	>5,000,000	50,000	NB	>−5.5	>2.2
H135A	5,000,000	>5,000,000	NB	>−5.5	>2.2
Q136A	>5,000,000	500,000	NB	>−5.5	>2.2
L137A	500	50–500	1.1	−8.1	−0.4
Q139A	>5,000,000	5,000,000	NB	>−5.5	>2.2
H141A	50–500	500	1.9	−7.8	−0.1
Y144A	500	500	1.4	−8.0	−0.3
G31S/S32P	>5,000,000	>5,000,000	1.4	−8.0	−0.3

[a] Mitogenic capacity of mutant TSST-1 molecules was estimated by the dose (picograms per milliliter) required to induce 50% of mitogenic activity compared with maximal activity of wild-type TSST-1.

[b] Affinity measurements were determined by surface plasmon resonance as described in *Materials and Methods.* The values for the individual ΔGs were calculated from the K_d obtained form surface plasmon resonance measurements according to the equation $\Delta G = -RT \ln (1/K_d)$, where R is the universal gas constant (−0.001986 kCal/mol·K), and T is the absolute temperature in Kelvin (298.15 K). $\Delta\Delta G = \Delta G_{mutant} - \Delta G_{wild\text{-}type}$.

[c] NB, binding not detected up to 100 μM human Vβ2.1Cβ.

capacity was defined as the SAG dose required to induce T cell proliferation that was 50% or greater than maximal proliferation induced by wild-type TSST-1 for each assay. Mitogenicity assays typically exhibited a clear dose response, where wild-type mitogenic capacity was achieved with SAG concentrations at 50 pg/ml, similar to previous data (30, 31, 39). For some protein preparations, the highest dose tested (5 μg/ml) occasionally had reduced activity or failed to stimulate proliferation. In this case, the lower dilutions that gave higher, dose-dependent mitogenic activities, were used for mitogenic capacity determination. Using these criteria, the mitogenic capacity of mutants Y13A and S15A was similar to that of wild-type TSST-1, while the mutants Y115A, L137A, H141A, and Y144A each displayed a slight loss of activity ($\geq$10-fold increase in mitogenic capacity) for both human and rabbit cells (Table II). The single-site mutants G16V, E132K, H135A, Q136A, and Q139A and the double-site mutant Y115A/W116G each had drastically reduced mitogenicity activity for human cells (Table II). The H135A, Q139A, and Y115A/W116G mutants each failed to produce significant proliferation for human lymphocytes above background levels at any concentration tested. Similar results were obtained for the control MHC class II binding mutant G31S/S32P. The W116A mutant displayed a strongly reduced ability to stimulate human cells ($\sim$1000-fold), yet maintained near wild-type activity for rabbit cells. Despite the Q136A and E132K mutants being inactive for human lymphocytes, both stimulated rabbit lymphocytes, but with reduced activity (Table II).

Direct binding of TSST-1 mutants to hVβ2.1

Since TSST-1 stimulates TCR Vβ2 (40), the binding affinity of each TSST-1 mutant to the hVβ2.1 chain was determined by surface plasmon resonance (BIAcore; Table II). This method has been successfully used to evaluate the stabilizing contribution of the TCR α-chain to the trimeric TCR/SAG/MHC complex (6, 41) and to map the free energy of the interactions between SEC3 and mouse Vβ8.2 by mutating both SEC3 (5) and Vβ8.2 TCR (42). Each mutated TSST-1 protein was coupled directly to the dextran matrix of sensor chips through the primary amino groups. Unglycosylated hVβ2.1 was injected, and concentration-dependent surface plasmon resonance profiles were recorded. A representative profile for wild-type TSST-1 and the SEB control, with a corresponding Scatchard plot, are shown in Fig. 1.

The Y13A, S15A, L137A, H141A, and Y144A mutants with similar or slightly reduced mitogenic profiles compared with that of wild-type TSST-1 also bound hVβ2.1 with affinities comparable to that of wild-type TSST-1. The Y115A mutant had a slightly reduced binding affinity (Table II), indicating a possible minor stabilizing interaction with hVβ2.1. Although L137V has been reported to cause a major decrease in mitogenic activity (30), the data presented here showed that L137A maintained both binding to hVβ2.1 and near wild-type mitogenic capacity. Therefore, we believe that Leu^{137} is not critical for interaction with the TCR. We also demonstrate that G16V, W116A, E132K, H135A, Q136A, and Q139A did not detectably bind to the hVβ2.1, providing direct evidence that the corresponding residues are critical for this interaction. Consistent with the G31S/S32P mutant being located within the MHC class II binding interface, this mutant maintained binding to hVβ2.1.

Induction of fever and toxicity of various TSST-1 mutants

Mutant proteins were examined in vivo for their ability to invoke fever responses and to induce lethal shock in two rabbit models of TSS (Table III). The presence of fever was taken as an average increase of $\geq\geq$0.5°C after 2 days of exposure to toxin by the miniosmotic pump model. Using these criteria, wild-type TSST-1

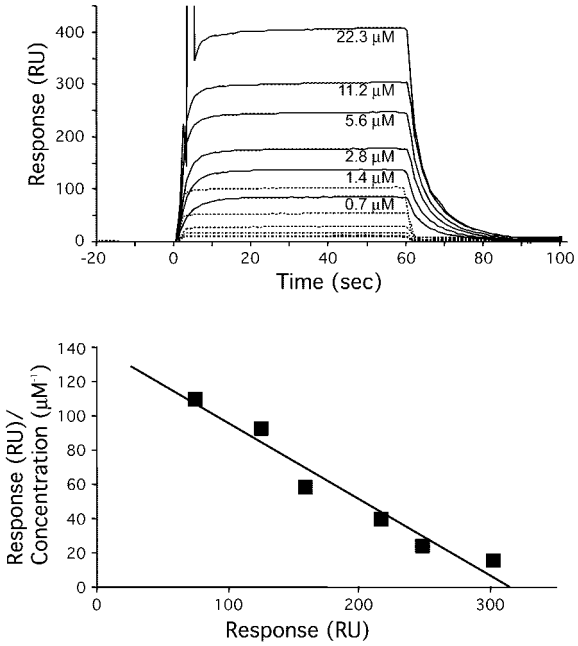

FIGURE 1. Evaluation of TSST-1/hVβ2.1 interaction by surface plasmon resonance analysis. *Top panel*, Equilibrium binding of hVb2.1 (concentration range, 0.7–22.3 μM) over a wild-type TSST-1 surface (957 RU immobilized; black curves) and a control SEB surface (1065 RU immobilized; dotted lines). *Bottom panel*, Scatchard analysis of equilibrium wild-type TSST-1 binding in the *top panel* after subtraction of binding to the control surface. The inverse of the absolute value of the slope represents a K_d of 2.3 μM ($r^2 = 0.96$).

and mutants Y13A, S15A, Y115A, and L137A were all pyrogenic. These toxins as well as the H141A mutant were also all lethal in both the miniosmotic pump and endotoxin enhancement models, indicating that individual residues were not critical for this activity despite slight decreases in mitogenic capacity or hVβ2.1 binding for Y115A, W116A, L137A, and H141A (Table II). Although the H141A mutant toxin did not cause significant fever, temperatures appeared to be elevated, yet did not reach the threshold criteria to be indicative of a fever response. This may indicate that the H141A mutant retained weak pyrogenic activity. The Y115A/W116G, Q139A, and Y144A mutants were nontoxic in the miniosmotic pump model of TSS, but only Y115A/W116G and Q139A mutants were nontoxic in the endotoxin enhancement model of TSS (Table III). Surprisingly, the Y144A mutant remained lethal in the endotoxin enhancement model of TSS. This result was remarkable because both models have always directly correlated for TSST-1 mutants and also for experiments with other staphylococcal and streptococcal SAGs. The inability of Y144A to cause death in the miniosmotic pump model initially led us to believe that residue Tyr^{144} was important for lethal activity. The miniosmotic pump model typically takes up to 5 days or more for the animal to develop shock, and we hypothesize that this protein is structurally unstable and has degraded to nontoxic levels by this time. The short time course leading to death in the endotoxin enhancement model ($<$24 h) and the relatively high doses of TSST-1 that the animals received for this model probably allowed for activity before toxin degradation. This may also be true for the lack of pyrogenic activity for this mutant. Alternatively, the endotoxin enhancement model may be more sensitive to TSST-1-mediated lethality than is the continuous infusion model. Finally, evaluation of the Q139A mutant, as assessed by the inability to proliferate T cells, induce fever, bind hVβ2.1, or demonstrate toxicity in two

Table III. *Pyrogenic and lethal activity of TSST-1 and various mutants*

Protein	Temperatures[a]			TSS Models (lethal/total)	
	Baseline ±SD	48 hr (± SD)	Δ°C	Miniosmotic pump[b]	Endotoxin enhancement[c]
Wild type	38.46 ± 0.18	39.46 ± 0.48	1.00	8/9	6/6
Y13A	38.87 ± 0.15	39.50 ± 0.20	0.63	3/3	3/3
S15A	38.63 ± 0.12	39.60 ± 0.36	0.97	3/3	3/3
G16V	39.18 ± 0.26	38.82 ± 0.36	−0.36	ND	ND
Y115A	37.90 ± 0.35	39.00 ± 0.72	1.10	4/6	3/3
W116A	38.30 ± 0.15	39.30 ± 0.72	0.51	3/3	3/3
Y115A/W116G	38.37 ± 0.45	38.27 ± 0.06	−0.10	0/3	0/3
L137A	38.53 ± 0.12	39.77 ± 0.78	1.24	3/3	3/3
Q139A	38.73 ± 0.21	38.53 ± 0.40	−0.20	0/3	0/3
H141A	38.83 ± 0.38	39.10 ± 0.92	0.27	3/3	3/3
Y144A	38.75 ± 0.26	38.82 ± 0.31	0.07	0/6	6/6
G31S/S32P	38.73 ± 0.35	39.23 ± 0.45	0.5	0/3	0/3

[a] Temperatures were taken prior to administration of miniosmotic pumps containing 200 μg of each toxin. Three or more rabbits were used for each protein. The induction of fever is taken as an increase in 0.5°C over a period of 4 h compared with baseline temperatures.

[b] Two hundred micrograms of each protein was administered in miniosmotic pumps.

[c] Rabbits were treated with 5 μg/ml/kg of TSST-1 or various mutant proteins administered i.v., and mortality was recorded over 10 days. After 4 h, 10 μg/ml/kg of endotoxin was given i.v., and mortality was recorded over 48 h.

rabbit models of lethal TSS, determined that residues Glu^{139} was also critical for TCR interaction and SAG function.

Discussion

The three-dimensional structures of several TCR β-chain/SAG complexes have now been reported, revealing the mechanism by which SAGs circumvent the normal mechanism for T cell activation (2). Although the interaction between TSST-1 and the human MHC class II molecule HLA-DR1 has been defined by cocrystal complex analysis (16), the interaction of TSST-1 with the TCR has not yet been fully characterized. Because TSST-1 is associated with most cases of *S. aureus* TSS, and this SAG represents a distinct subgroup among the pyrogenic toxin SAGs (3), a complete understanding of the interaction between TSST-1 and the TCR is highly desirable. Furthermore, the location of the predicted TCR binding domain of TSST-1 appears to be distinct from the now well characterized TCR binding domains of SEB, SEC, SPE A, and SPE C.

Two of the mutated residues in TSST-1 (Leu^{137} and Tyr^{144}) appear to be universally conserved among all the characterized pyrogenic toxin SAGs, and both these residues are buried in the TSST-1 crystal structure. The failure of L137A and Y144A to affect functional activity was not unexpected, yet this may imply that these and possibly other universally conserved residues are not important for ligand formation. In conjunction with our current data for Tyr^{144}, this finding is complementary to a previous double mutant (H141A/Y144A) that was found to have no mitogenic activity or toxicity in an in vivo rabbit model (27). The H141A/Y144A mutant also lost the ability to be recognized by a mAb, suggesting conformational changes or degradation. We believe that the combined effects of mutating these two residues resulted in a net loss of binding energetics sufficient to cause the loss of function. This may be similar to the double-mutant Y115A/W116G constructed in this study. The failure of the L137A mutation to largely inhibit mitogenicity is, however, in contradiction to earlier results (30). It was previously determined that L137V had dramatically decreased T cell stimulatory activity, but maintained binding to HLA-DR. The majority of residue Leu^{137} is not surface exposed, and it is possible that the Leu→Val mutation imposed a localized steric alteration within the TCR binding region. Indeed, Hurley et al. (30) originally hypothesized that this may explain the inactivity of this mutant. The G31S/S32P mutant behaved as expected in all experiments, including the ability to bind hVβ2.1, although this protein was not mitogenic or pyrogenic, and these results further demonstrate that TSST-1 interaction with the MHC class II molecule is critical for each of these functional activities, including the development of lethal shock.

The slight decrease in hVβ2.1 binding seen for mutations at positions Tyr^{13}, Tyr^{115}, and His^{141} may indicate minor involvement in the TCR/TSST-1 complex, probably through stabilizing interactions. Based on the cocrystal structure of SEC3 in contact with the mouse 14.3.d β-chain (21), the mutation of all SEC3 residues involved in contact with the β-chain revealed that only two of 12 residues (N23A, Q210A) completely lost detectable binding using their criteria for stimulatory capacity, while a third mutation (F176A) had barely detectable mitogenic activity (5). Most other SEC3 mutations did show more intermediate decreases in stimulatory capacity, which we did not observe for the TSST-1 mutants, although three SEC3 mutants showed similar minor decreases in mitogenic activity (5). These residues (Gly^{102}, Lys^{103}, and Gly^{106} in SEC3) are located on the flexible disulfide loop and do not form hydrogen bonds with the 14.3.d TCR (21). It is likely that Tyr^{13}, Tyr^{115}, and His^{141} may participate in similar weak bonding arrangements that are not critical for functional interaction, but contribute to overall binding energetics.

SAG activity leads to massive T cell stimulation and proliferation, and it is generally believed that cytokine release as a result of this activity is responsible for the most severe consequences of TSS. Alternatively, the role of SAGs in autoimmune disorders is probably due to the proliferation of autoreactive T cell subsets. Although mitogenicity and lethality are clearly affiliated, some evidence indicates that superantigenic activity and lethality are separable biological properties. The Q136A mutation of TSST-1 was previously reported to maintain superantigenicity (~60%) for rabbit T cells (but not human T cells), although lethal activity in rabbits was not exhibited at any dose tested (31). The three-dimensional structure of the Q136A mutant has been determined (32). This mutation caused a dramatic alteration in the β7-β9 loop, which covers the central α helix. Because this mutation retained some activity for rabbit T cells, but lost lethal activity in rabbits, the authors hypothesized that the β7-β9 loop may mediate the ability of the toxin to induce lethality (32). Significantly, residues Tyr^{115} and Trp^{116} reside in this loop. However, using our current criteria, the Q136A mutation would result in a mitogenic capacity

of 500,000 pg/ml for rabbit splenocytes, indicating a >1,000-fold reduction in activity. This mitogenic capacity may predict a threshold of SAG activity required for lethal activity induced through cytokine release. This would predict high levels (>2 mg/rabbit) of Q136A to induce T cell-mediated lethal shock. The ability of W116A, E132K, and Q136A to have much stronger mitogenic activity for rabbit cells compared with human cells may also indicate a separate Vβ-chain that is stimulated in the rabbit or may reflect differences in the rabbit equivalent to hVβ2.1. This hypothesis remains a possibility due to the close location of residues Glu^{132} and Glu^{136} in TSST-1 and probably explains the residual activity for rabbit cells seen with these two mutants.

Since many SAGs have affinities for both TCR and MHC in the micromolar range (2), it can be predicted that most SAG trimeric complexes would be unbound at physiological concentrations (43). Andersen et al. (6) have elegantly shown that the TCR α-chain interacts with the MHC β-chain to stabilize the trimeric complex involving SEB. Although, the TCR/SPE C/MHC class II model predicts that in this interaction SAG acts as a bridge without any direct interactions between TCR and MHC class II, SPE C contains a high affinity ($K_d = \sim 4 \times 10^{-8}$ M), zinc-dependent, MHC class II binding domain (19), and small changes in MHC affinity can overcome larger increases in TCR affinity (5). Thus, it appears that the high affinity MHC binding site can circumvent the requirement for stabilizing interactions between the TCR and MHC class II (19). Mutagenesis of SEC3 showed a direct correlation between the affinity of SEC3 for the TCR β-chain and mitogenicity (5). Recently, phage display was used to engineer SEC3 variants in the disulfide loop with increased affinities to the α/β TCR revealing that increasing affinity of the SEC3/TCR complex above that normally seen with SAG/TCR interactions resulted in increased T cell activation (8). These studies each indicate a direct correlation between ligand affinity and potency of bacterial SAG/TCR complexes. This correlation also exists for TSST-1 with hVβ2.1.

For each of the cocrystal structures involving bacterial SAGs (SEB, SEC, SPE A, and SPE C) and their corresponding TCR β-chains (21–23), each SAG binds the TCR in the cleft between the large and small domains, although SPE C engages the TCR in a different orientation compared with SEB, SEC, and SPE A. To illustrate the hVβ2.1 binding domain of TSST-1, Fig. 2 shows ribbon (Fig. 2*A*) and space-filling (Fig. 2*B*) diagrams, with residues important for hVβ2.1 interaction highlighted. The six residues of TSST-1 that are individually critical for functional interaction are shown in red. The residue that partially inhibited binding is highlighted in blue, and residues believed to play insignificant or minor stabilizing roles are shown in green. Our mutagenesis data presented here show the location of the hVβ2.1 binding domain of TSST-1 to exist in a groove formed between the central and N-terminal α helixes, adjacent to the β7-β9 loop. The location of the hVβ2.1 binding domain of TSST-1 is in sharp contrast to known TCR β-chain binding regions of SEB (Fig. 2*C*), SPE A (Fig. 2*D*), and SPE C (Fig. 2*E*) (22, 23).

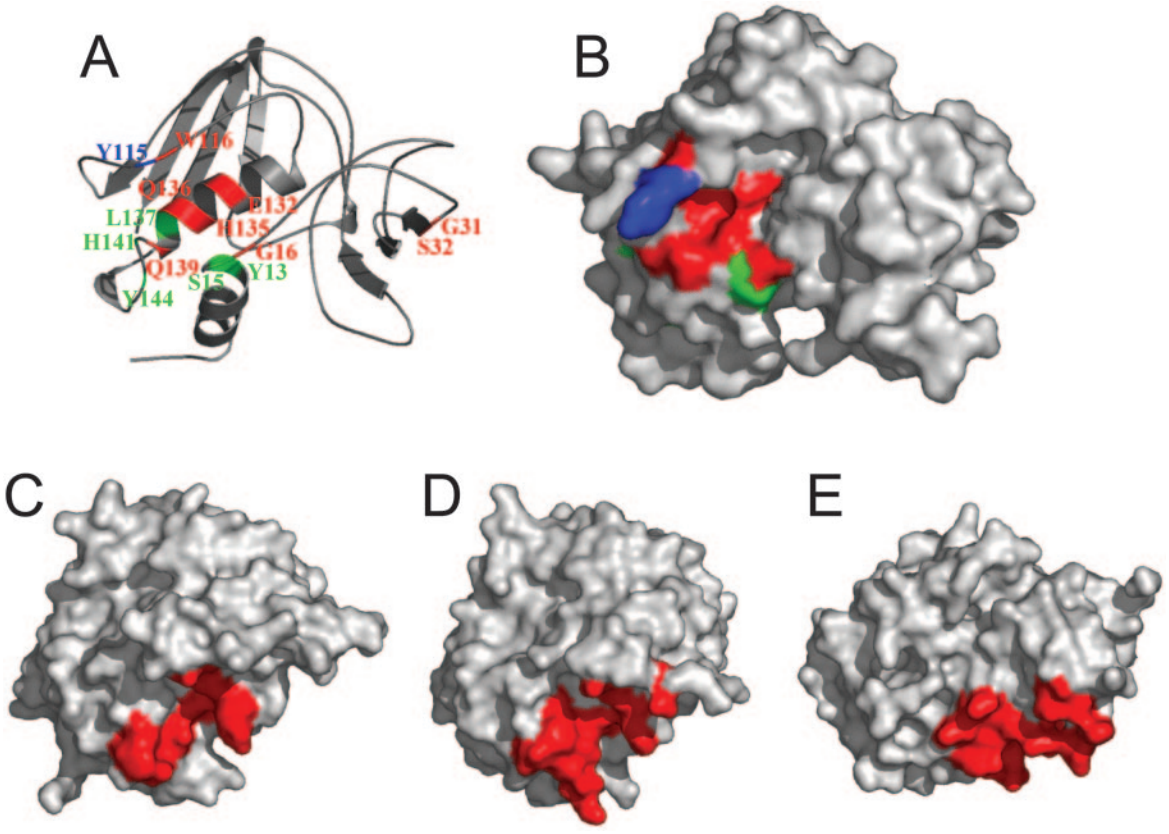

FIGURE 2. Mapping the functionality of TSST-1 residues to its three-dimensional structure and comparison with other SAG TCR β-chain contact residues. *A*, Ribbon diagram of TSST-1, highlighting the location and functional effect of mutations. Functionality is color-coded in the following way: TSST-1 mutations that result in abrogation of its complex with hVβ2.1 ($\Delta\Delta G > 2$ kcal/mol) are red, TSST-1 mutations that partially inhibit binding to hVβ2.1 ($1 < \Delta\Delta G < 2$ kcal/mol) are blue, and TSST-1 mutations that do not affect interaction with hVβ2.1 ($\Delta\Delta G < 1$ kcal/mol) are green. *B*, Mutations mapped to the molecular surface of TSST-1 reveal that residues important for complex formation with hVβ2.1 are predominantly clustered together within the groove formed between two α helices. Color-coding of functionality is the same as in *A*. Molecular surfaces of SAGs structurally aligned with TSST-1 to indicate the SEB/mVβ8.2 (*C*), SPE A/mVβ8.2 (*D*), and SPE C/hVβ2.1 (*E*) interactions, with contact residues colored red (22, 23). The TCR β-chain binding surface of SEC3 is highly similar to SEB and is not shown (21).

From our data and based on the previous cocrystal structure of TSST-1 complexed with HLA-DR1 (16), we have constructed a hypothetical model of the tenary complex (Fig. 3). In general, the TSST-1 ternary model fits the standard wedge model for TCR binding (Fig. 3) (21), yet there are important differences. For the model the most unique region of hVβ2.1 (the CDR2 loop) was aligned with the TSST-1 region that has the greatest effect on binding according to the mutagenesis data. The CDR2 loop fits nicely into the pocket outlined in red on the TSST-1 molecular surface (Fig. 2*B*), and the CDR3 loop wraps around underneath the second α helix and fits into the depression bordered by the N-terminal helix. In this position, CDR2 of the TCR α-chain and the MHC β subunit may result in a small interface similar to that seen in the SEB/SEC3 ternary complexes. Because TSST-1 does not contain the high affinity, zinc-dependent, MHC class II binding domain, it is likely that the TCR/MHC interaction in the TSST-1 complex is necessary for complex stabilization. It is also possible that TSST-1 represents a hybrid ternary complex where (like SEB/SEC3 and unlike SpeC) TSST-1 acts as a wedge between MHC and TCR, allowing for direct TCR α-chain/MHC β-chain contacts, yet unlike the SEB/SEC3 trimeric complexes and similar to the SPE C trimeric complex, the CDR3 loop of hVb2.1 is probably involved in direct SAG-TCR molecular interactions that could contribute to the TCR Vβ specificity of TSST-1. Cocrystallization of TSST-1 with the TCR β-chain will be necessary to confirm our current results and help further our overall understanding of this important interaction.

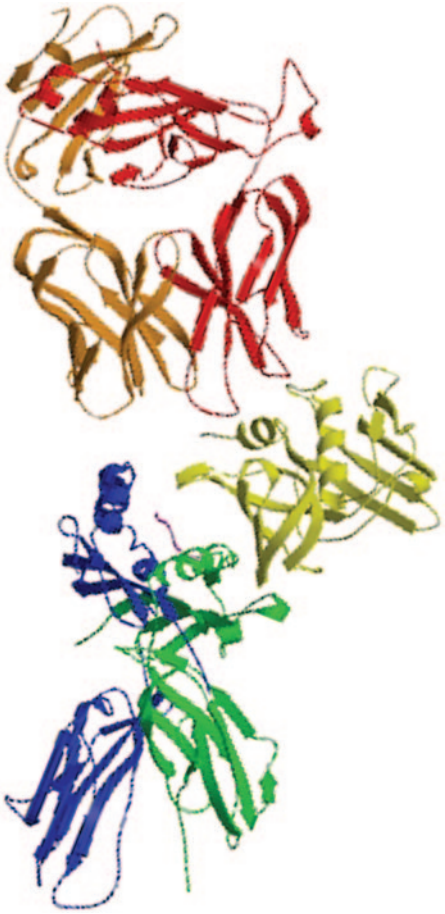

FIGURE 3. Hypothetical model of the TSST-1-dependent T cell signaling complex. The model was created by aligning the TSST-1 molecular surface important for hVβ2.1 binding with the most unique region of the hVβ2.1 structure, the CDR2 loop, a likely scenario considering that TSST-1 activates hVβ2.1$^+$ T cells exclusively. Colors are as follows: TSST-1, yellow; hVβ2.1, red; TCR α-chain, orange; MHC α subunit, green; MHC β subunit, blue; antigenic peptide, gray. This model predicts a possible direct interaction between the TCR α-chain and the MHC β subunit (intersection of blue and orange domains), much like in the SEB- and SEC3-dependent T cell signaling complexes (6, 22, 44).

References

1. Marrack, P., and J. Kappler. 1990. The staphylococcal enterotoxins and their relatives. *Science 248:705.*
2. Li, H., A. Llera, E. L. Malchiodi, and R. A. Mariuzza. 1999. The structural basis of T cell activation by superantigens. *Annu. Rev. Immunol. 17:435.*
3. McCormick, J. K., J. M. Yarwood, and P. M. Schlievert. 2001. Bacterial superantigens and toxic shock syndrome: an update. *Annu. Rev. Microbiol. 55:77.*
4. Malchiodi, E. L., E. Eisenstein, B. A. Fields, D. H. Ohlendorf, P. M. Schlievert, K. Karjalainen, and R. A. Mariuzza. 1995. Superantigen binding to a T cell receptor β chain of known three-dimensional structure. *J. Exp. Med. 182:1833.*
5. Leder, L., A. Llera, P. M. Lavoie, M. I. Lebedeva, H. Li, R. P. Sekaly, G. A. Bohach, P. J. Gahr, P. M. Schlievert, K. Karjalainen, et al. 1998. A mutational analysis of the binding of staphylococcal enterotoxins B and C3 to the T cell receptor β chain and major histocompatibility complex class II. *J. Exp. Med. 187:823.*
6. Andersen, P. S., P. M. Lavoie, R. P. Sekaly, H. Churchill, D. M. Kranz, P. M. Schlievert, K. Karjalainen, and R. A. Mariuzza. 1999. Role of the T cell receptor α chain in stabilizing TCR-superantigen-MHC class II complexes. *Immunity 10:473.*
7. Redpath, S., S. M. Alam, C. M. Lin, A. M. O'Rourke, and N. R. Gascoigne. 1999. Cutting edge: trimolecular interaction of TCR with MHC class II and bacterial superantigen shows a similar affinity to MHC:peptide ligands. *J. Immunol. 163:6.*
8. Andersen, P. S., C. Geisler, S. Buus, R. A. Mariuzza, and K. Karjalainen. 2001. Role of TCR-ligand affinity in T cell activation by bacterial superantigens. *J. Biol. Chem. 7:7.*
9. White, J., A. Herman, A. M. Pullen, R. Kubo, J. W. Kappler, and P. Marrack. 1989. The Vβ-specific superantigen staphylococcal enterotoxin B: stimulation of mature T cells and clonal deletion in neonatal mice. *Cell 56:27.*
10. Bergdoll, M. S., B. A. Crass, R. F. Reiser, R. N. Robbins, and J. P. Davis. 1981. A new staphylococcal enterotoxin, enterotoxin F, associated with toxic-shock-syndrome *Staphylococcus aureus* isolates. *Lancet 1:1017.*
11. Schlievert, P. M., K. N. Shands, B. B. Dan, G. P. Schmid, and R. D. Nishimura. 1981. Identification and characterization of an exotoxin from *Staphylococcus aureus* associated with toxic-shock syndrome. *J. Infect. Dis. 143:509.*
12. Bohach, G. A., B. N. Kreiswirth, R. P. Novick, and P. M. Schlievert. 1989. Analysis of toxic shock syndrome isolates producing staphylococcal enterotoxins B and C1 with use of southern hybridization and immunologic assays. *Rev. Infect. Dis. 11(Suppl. 1):S75.*
13. Schlievert, P. M., L. M. Jablonski, M. Roggiani, I. Sadler, S. Callantine, D. T. Mitchell, D. H. Ohlendorf, and G. A. Bohach. 2000. Pyrogenic toxin superantigen site specificity in toxic shock syndrome and food poisoning in animals. *Infect. Immun. 68:3630.*
14. Prasad, G. S., C. A. Earhart, D. L. Murray, R. P. Novick, P. M. Schlievert, and D. H. Ohlendorf. 1993. Structure of toxic shock syndrome toxin 1. *Biochemistry 32:13761.*
15. Acharya, K. R., E. F. Passalacqua, E. Y. Jones, K. Harlos, D. I. Stuart, R. D. Brehm, and H. S. Tranter. 1994. Structural basis of superantigen action inferred from crystal structure of toxic-shock syndrome toxin-1. *Nature 367:94.*
16. Kim, J., R. G. Urban, J. L. Strominger, and D. C. Wiley. 1994. Toxic shock syndrome toxin-1 complexed with a class II major histocompatibility molecule HLA-DR1. *Science 266:1870.*
17. Jardetzky, T. S., J. H. Brown, J. C. Gorga, L. J. Stern, R. G. Urban, Y. I. Chi, C. Stauffacher, J. L. Strominger, and D. C. Wiley. 1994. Three-dimensional structure of a human class II histocompatibility molecule complexed with superantigen. *Nature 368:711.*
18. Wen, R., G. A. Cole, S. Surman, M. A. Blackman, and D. L. Woodland. 1996. Major histocompatibility complex class II-associated peptides control the presentation of bacterial superantigens to T cells. *J. Exp. Med. 183:1083.*
19. Li, Y., H. Li, N. Dimasi, J. K. McCormick, R. Martin, P. Schuck, P. M. Schlievert, and R. A. Mariuzza. 2001. Crystal structure of a superantigen bound to the high-affinity, zinc-dependent site on MHC class II. *Immunity 14:93.*
20. Petersson, K., M. Hakansson, H. Nilsson, G. Forsberg, L. A. Svensson, A. Liljas, and B. Walse. 2001. Crystal structure of a superantigen bound to MHC class II displays zinc and peptide dependence. *EMBO J. 20:3306.*
21. Fields, B. A., E. L. Malchiodi, H. Li, X. Ysern, C. V. Stauffacher, P. M. Schlievert, K. Karjalainen, and R. A. Mariuzza. 1996. Crystal structure of a T-cell receptor β-chain complexed with a superantigen. *Nature 384:188.*
22. Li, H., A. Llera, D. Tsuchiya, L. Leder, X. Ysern, P. M. Schlievert, K. Karjalainen, and R. A. Mariuzza. 1998. Three-dimensional structure of the complex between a T cell receptor β chain and the superantigen staphylococcal enterotoxin B. *Immunity 9:807.*
23. Sundberg, E. J., H. Li, A. S. Llera, J. K. McCormick, J. Tormo, P. M. Schlievert, K. Karjalainen, and R. A. Mariuzza. 2002. Structures of two streptococcal superantigens bound to TCR β chains reveal diversity in the architecture of T cell signaling complexes. *Structure 10:687.*
24. Morita, C. T., H. Li, J. G. Lamphear, R. R. Rich, J. D. Fraser, R. A. Mariuzza, and H. K. Lee. 2001. Superantigen recognition by $\gamma\delta$ T cells: SEA recognition site for human Vγ2 T cell receptors. *Immunity 14:331.*

25. Hodtsev, A. S., Y. Choi, E. Spanopoulou, and D. N. Posnett. 1998. Mycoplasma superantigen is a CDR3-dependent ligand for the T cell antigen receptor. *J. Exp. Med. 187:319.*
26. Blanco, L., E. M. Choi, K. Connolly, M. R. Thompson, and P. F. Bonventre. 1990. Mutants of staphylococcal toxic shock syndrome toxin 1: mitogenicity and recognition by a neutralizing monoclonal antibody. *Infect. Immun. 58:3020.*
27. Bonventre, P. F., H. Heeg, C. Cullen, and C. J. Lian. 1993. Toxicity of recombinant toxic shock syndrome toxin 1 and mutant toxins produced by *Staphylococcus aureus* in a rabbit infection model of toxic shock syndrome. *Infect. Immun. 61:793.*
28. Deresiewicz, R. L., J. Woo, M. Chan, R. W. Finberg, and D. L. Kasper. 1994. Mutations affecting the activity of toxic shock syndrome toxin-1. *Biochemistry 33:12844.*
29. Murray, D. L., G. S. Prasad, C. A. Earhart, B. A. Leonard, B. N. Kreiswirth, R. P. Novick, D. H. Ohlendorf, and P. M. Schlievert. 1994. Immunobiologic and biochemical properties of mutants of toxic shock syndrome toxin-1. *J. Immunol. 152:87.*
30. Hurley, J. M., R. Shimonkevitz, A. Hanagan, K. Enney, E. Boen, S. Malmstrom, B. L. Kotzin, and M. Matsumura. 1995. Identification of class II major histocompatibility complex and T cell receptor binding sites in the superantigen toxic shock syndrome toxin 1. *J. Exp. Med. 181:2229.*
31. Murray, D. L., C. A. Earhart, D. T. Mitchell, D. H. Ohlendorf, R. P. Novick, and P. M. Schlievert. 1996. Localization of biologically important regions on toxic shock syndrome toxin 1. *Infect. Immun. 64:371.*
32. Earhart, C. A., D. T. Mitchell, D. L. Murray, D. M. Pinheiro, M. Matsumura, P. M. Schlievert, and D. H. Ohlendorf. 1998. Structures of five mutants of toxic shock syndrome toxin-1 with reduced biological activity. *Biochemistry 37:7194.*
33. Blomster-Hautamaa, D. A., B. N. Kreiswirth, J. S. Kornblum, R. P. Novick, and P. M. Schlievert. 1986. The nucleotide and partial amino acid sequence of toxic shock syndrome toxin-1. *J. Biol. Chem. 261:15783.*
34. Chang, S., and S. N. Cohen. 1979. High frequency transformation of *Bacillus subtilis* protoplasts by plasmid DNA. *Mol. Gen. Genet. 168:111.*
35. Parsonnet, J., Z. A. Gillis, A. G. Richter, and G. B. Pier. 1987. A rabbit model of toxic shock syndrome that uses a constant, subcutaneous infusion of toxic shock syndrome toxin 1. *Infect. Immun. 55:1070.*
36. Schlievert, P. M. 1982. Enhancement of host susceptibility to lethal endotoxin shock by staphylococcal pyrogenic exotoxin type C. *Infect. Immun. 36:123.*
37. Wells, J. A. 1991. Systematic mutational analyses of protein-protein interfaces. *Methods Enzymol. 202:390.*
38. Kum, W. W., J. A. Wood, and A. W. Chow. 1996. A mutation at glycine residue 31 of toxic shock syndrome toxin-1 defines a functional site critical for major histocompatibility complex class II binding and superantigenic activity. *J. Infect. Dis. 174:1261.*
39. Prasad, G. S., R. Radhakrishnan, D. T. Mitchell, C. A. Earhart, M. M. Dinges, W. J. Cook, P. M. Schlievert, and D. H. Ohlendorf. 1997. Refined structures of three crystal forms of toxic shock syndrome toxin-1 and of a tetramutant with reduced activity. *Protein Sci. 6:1220.*
40. Kotzin, B. L., D. Y. Leung, J. Kappler, and P. Marrack. 1993. Superantigens and their potential role in human disease. *Adv. Immunol. 54:99.*
41. Seth, A., L. J. Stern, T. H. Ottenhoff, I. Engel, M. J. Owen, J. R. Lamb, R. D. Klausner, and D. C. Wiley. 1994. Binary and ternary complexes between T-cell receptor, class II MHC and superantigen in vitro. *Nature 369:324.*
42. Churchill, H. R., P. S. Andersen, E. A. Parke, R. A. Mariuzza, and D. M. Kranz. 2000. Mapping the energy of superantigen staphylococcus enterotoxin C3 recognition of an α/β T cell receptor using alanine scanning mutagenesis. *J. Exp. Med. 191:835.*
43. Proft, T., and J. Fraser. 1998. Superantigens: just like peptides only different. *J. Exp. Med. 187:819.*
44. Andersen, P. S., P. Schuck, E. J. Sundberg, C. Geisler, K. Karjalainen, and R. A. Mariuzza. 2002. Quantifying the energetics of cooperativity in a ternary protein complex. *Biochemistry 41:5177.*